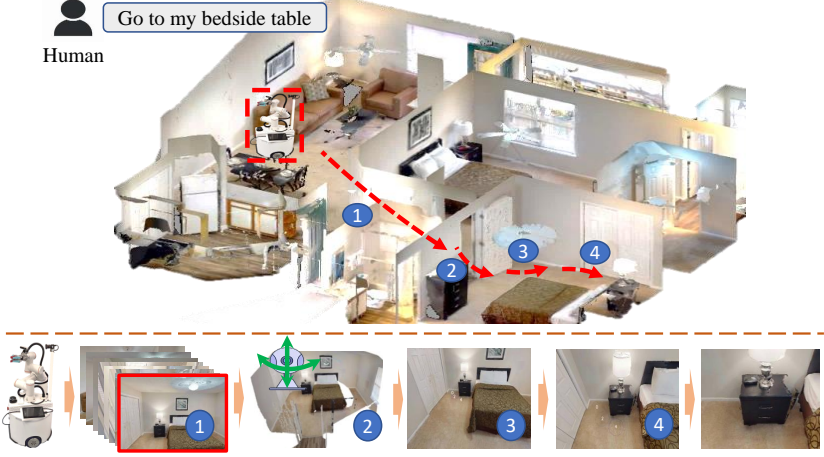
# Navi2Gaze: Leveraging Foundation Models for Navigation and Target Gazing

Jun Zhu<sup>1,\*</sup>, Zihao Du<sup>1,\*</sup>, Haotian Xu<sup>1</sup>, Fengbo Lan<sup>1</sup>, Zilong Zheng<sup>2</sup>, Bo Ma<sup>3</sup>, Shengjie Wang<sup>4,†</sup>, and Tao Zhang<sup>1,†</sup>, Fellow, IEEE

<sup>1</sup> Department of Automation, Tsinghua University.

Abstract: Task-aware navigation continues to be a challenging area of research, especially in scenarios involving open vocabulary. Previous studies primarily focus on finding suitable locations for task completion, often overlooking the importance of the robot's pose. However, the robot's orientation is crucial for successfully completing tasks because of how objects are arranged (e.g., to open a refrigerator door). Humans intuitively navigate to objects with the right orientation using semantics and common sense. For instance, when opening a refrigerator, we naturally stand in front of it rather than to the side. Recent advances suggest that Vision-Language Models (VLMs) can provide robots with similar common sense. Therefore, we develop a VLM-driven method called Navigation-to-Gaze (Navi2Gaze) for efficient navigation and object gazing based on task descriptions. This method uses the VLM to score and select the best pose from numerous candidates automatically. In evaluations on multiple photorealistic simulation benchmarks, Navi2Gaze significantly outperforms existing approaches and precisely determines the optimal orientation relative to target objects.

**Keywords:** Navigation, VLM, Semantic Scene Understanding



Robot Scene navigation Space reconstruction First decision Second decision Gazing object

**Figure 1: Workflow of Navi2Gaze:** Upon receipt of user instructions, the robot employs a Visual Language Model (VLM) to identify the scene encompassing the target object and subsequently navigates to the corresponding region. Utilizing an RGBD camera, the robot reconstructs the spatial environment surrounding the target object. The area around the target is then divided into location candidates, and through a two-step scoring process, the robot navigates to the vicinity of the target. Finally, the robot's posture is adjusted to gaze at the target object.

<sup>&</sup>lt;sup>2</sup> Beijing Institute for General Artificial Intelligence.

<sup>&</sup>lt;sup>3</sup> Chengdu Aircraft Design & Research Institute.

<sup>&</sup>lt;sup>4</sup> Institute for Interdisciplinary Information Sciences (IIIS), Tsinghua University.

### 1 Introduction

The capability of zero-shot object navigation (ZSON) is deemed essential for the effective operation of home-assistance robots. Current research commonly views final locations close to targets as the measure of successful navigation. In practice, an appropriate orientation relative to the object, often overlooked by existing methods, is crucial for enhancing subsequent operations [1–3]. Consider an intuitive example: when a navigation system directs robots only to the refrigerator without addressing the need to open its door, the robots may end up positioned at an impractical side or back, thereby hindering the smooth execution of further actions. Similarly, for a task like sitting on a sofa, simply arriving nearby is inadequate; the robot must be properly aligned to face the sofa and positioned to sit down comfortably. Although 6D object pose estimation can be obtained from recent work [4–8], the model still struggles to choose the appropriate orientation for specific tasks.

Recently, Visual language models (VLMs) have emerged as a promising approach for understanding the world through images and text inputs, learning to represent these perceptions by projecting them into a linguistic space [9–11]. Due to the lack of spatial understanding, it is impractical for VLMs to directly generate navigation trajectories in text form. Current state-of-the-art navigation algorithms[12–14] predominantly utilize VLMs for common sense reasoning and image-level visual perception[15, 16]. These models process inputs ranging from original images to those augmented with colorful boxes or segmentation masks[17–19]. While these visual prompts enable VLMs to guide robots to the vicinity of the target object, they can not directly provide the precise orientation required for subsequent tasks, primarily due to the absence of 3D spatial projection information. Thus, the question then arises: how can we use the common sense of VLMs to develop a task-aware navigation system that can navigate to the target object with the correct orientation?

To address this challenge, we propose a VLM-driven Navigation-to-Gazing method, named Navi2Gaze. Our method first provides potential candidates (target scenes, regions of the robot, and objects) to the VLM, then uses a coarse-to-fine mechanism to score candidates, and finally chooses the best pose for the robot. For instance, given the instruction "open the refrigerator," VLMs can be prompted to: 1) Select the optimal scene where the refrigerator is visible, 2) Navigate to the region corresponding to this image, and 3) Identify the ideal position near the refrigerator that facilitates easy opening. Navigation is executed by the underlying path planning algorithm, while VLMs function as the robot's decision-making brain. An illustrative diagram and a subset of tasks we considered are shown in Fig. 1. In summary, our contributions are threefold:

- Navigation with Gazing at the Object We propose a universal framework that navigates the robot toward the target object with the appropriate orientation, thus facilitating the success of further manipulation.
- VLM-based Scoring Function To make full use of the common sense in VLMs, we design a VLM-based scoring function that automatically generates scores for the robot to choose the optimal pose, using visual observations with annotated candidates. We showcase its zero-shot generalization capabilities for open-set instructions involving open-set objects across a range of daily navigation tasks.
- Navigation without a 3D Semantic Map Our method leverages a VLM-driven navigation policy to choose the best pose for the robot, given only a few visual observations and a simple 2D navigation map.

#### 2 Related Works

#### 2.1 Open-Vocabulary Object Navigation

Most previous studies have employed contrastively trained visual language models (VLMs), such as GLIP[15] and CLIP[16], to address the open-vocabulary object navigation challenge. These models, trained on image-language associations, facilitate open-vocabulary image understanding and object detection. For instance, ZSON [12] utilizes CLIP to map image-goals (e.g., a picture of the

sink) and object-goals (e.g., "sink") into a semantic-goal embedding space. This approach facilitates training that enables agents to identify objects described in natural language. An ensemble of ViLD[20] and CLIP is utilized in NLMap[21] to extract image embeddings that are queryable via text. VLMaps[13] integrates pretrained visual-language features, extracted by LSeg[22], with a 3D reconstruction of the physical world to generate a spatial map representation. Recently, advancements in VLMs have demonstrated such robust vision-language understanding capabilities that they may potentially replace visual language models. Furthermore, we have discovered that a few images can capture nearly all elements within a scene, allowing us to forego the creation of a semantic map for simplicity.

# 2.2 Visual Prompting

Despite impressive zero-shot transfer capabilities in image-level visual perception, recent studies[17, 18, 23, 24, 19] indicate that both VLMs and LLMs exhibit limited effectiveness in instance-level tasks requiring precise localization and recognition. Therefore, researchers suggest that integrating visual prompts, such as colorful boxes, circles, precise semantic markers, and highlighted regions, can enhance the models' ability to recognize objects of interest. For example, SoM[17] employs SEEM[25] or SAM[26] to partition an image into regions with varying granularity, overlaying these regions with a variety of markers such as alphanumerics, masks, and boxes. Additionally, FGVP[18] utilizes precise semantic masks of target instances derived via SAM. To generate fine-grained masks, the variants[27, 28] of SAM, PerSAM[29], and SAM-PT[30], can also be employed. Our approach employs visual prompts, similar to SoM, to select the optimal image in which the target object is visible. Besides, it draws colorful circles near the target on the image, enabling VLMs to identify the optimal position near the target object through a scoring mechanism.

#### 2.3 LLMs for Visual Navigation

The perceptual and decision-making capabilities of large language models (LLMs) significantly enhance robotic navigation autonomy [31, 10]. For instance, L3MVN [32] uses LLMs to identify relevant areas from a semantic map for better exploration. ESC [33] leverages LLMs for commonsense reasoning about spatial relations between goal objects and common objects or rooms. LGX [34] generates prompts from extracted object labels, guiding the navigation path. LFG [35] uses positive and negative prompts for multiple samplings, providing scores as heuristics for the search algorithm. PixNav [14] combines LLMs and VLMs to analyze panoramic images and determine room-level relationships, segment images, and guide robotic movements. StructNav [36] uses language and scene-based priors to semantically score geometry-based boundaries, aiding in reasoning about promising search areas. LM-Nav [37] uses three pretrained models for planning: a large language model for landmark extraction, a vision-language model for localization, and a vision navigation model for execution. We adopt the use of VLMs to improve object navigation efficiency. Unlike previous studies, we develop visual prompts that guide VLMs to accurately locate target objects and select the optimal orientation.

# 3 Methodology

Leveraging the image recognition and natural language understanding capabilities of VLMs, a universal framework is introduced to guide robots towards the target object in the appropriate orientation. This framework effectively reduces the motion gap between navigation and manipulation, enhancing the efficiency and flexibility of robots operating in home environments.

A graphical overview of the framework is shown in Figure 2. Our method processes a natural language query (e.g., "open the refrigerator"), locates the queried object within a set  $S = \{I_i\}_1^N$  of N images captured by the robot, navigates to the image location with the object, selects an optimal nearby position, and moves to this position. We assume a 2D occupancy map  $\mathcal{M}_o$  of the environment and an image set S covering the scene. This is feasible in indoor settings where exploration can be done in one go. We simplify the navigation task to a search problem: the robot proposes subgoals,

evaluates them, and uses a search algorithm to plan the path. The core of Navi2Gaze is scoring subgoal proposals from coarse to fine. First, it selects the image where the object is most visible, then it chooses the best nearby position to ensure optimal orientation.

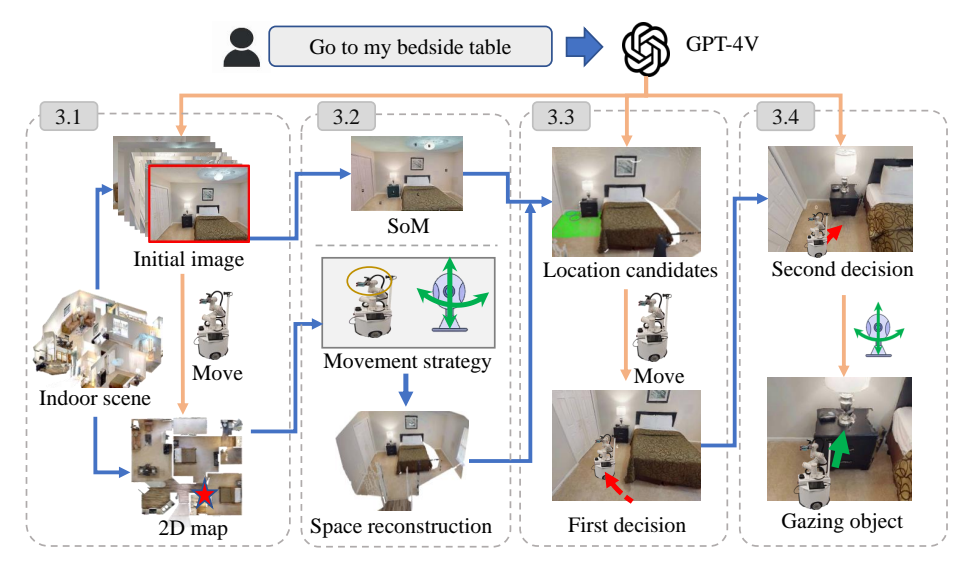


Figure 2: Framework of Navi2Gaze: The Navi2Gaze framework has four main components: *Identification of Target Scene*, *Reconstruction of Task-aware Space*, *Generation of Location Candidates*, and *Sequential Decisions for Gazing Objects*. 1. *Identification of Target Scene*: The robot uses GPT-4V to find and navigate to the target object using image sequences. 2. *Reconstruction of Task-aware Space*: The robot moves its camera to map the scene around the target object. 3. *Generation of Location Candidates*: Self-organizing Maps (SoM) and GPT-4V identify the target and suggest possible regions for the robot to position itself. 4. *Sequential Decisions for Gazing Objects*: GPT-4V scores these regions and directs the robot to the best position for observing the target.

#### 3.1 Identification of Target Scene

Navigating to the photographic location of an image that includes the target object, using a set of scene images and a 2D occupancy map, constitutes the first critical step of our method. This strategy ensures that the target object appears within the robot's field of view. Specifically, our aim is to develop a scoring function utilizing a VLM that processes the image set  $\mathcal{S}$  along with the goal query q as inputs. This function is designed to compute the task-relevant probability  $p(I_i, q, \mathcal{S})$  for each image  $I_i$  within  $\mathcal{S}$ . To ensure precise indexing of VLMs, each image is marked with a unique red number in the upper left corner. We adopt a chain-of-thought prompting approach, which initially guides the VLM to identify images containing the queried object, then to discern the clearest image. With the pose of the selected image determined, we project its 3D position onto a 2D occupancy map, thus establishing the 2D goal. This goal is then pursued using a 2D navigation system, effectively bridging the gap between image-based identification and physical navigation tasks.

#### 3.2 Reconstruction of Task-aware Space

Obtaining extensive and up-to-date spatial information around the target object is the core prerequisite for guiding robotic navigation to the optimal orientation position. To this end, we divide the process into two components: target object recognition and extensive point cloud collection.

To accurately ascertain the location of the queried object, we employ the methodology used in SoM[17]. Initially, segmentation models such as SEEM[25] and SAM[26] are utilized to partition an image into regions based on semantic content. These regions are then distinctly colored and superimposed with various numeric markers. Instead of relying solely on the marked image as in the SoM approach, we pair the original image with the marked, color-enhanced image before feeding them to the VLM. This dual-input strategy enhances the VLM's ability to more effectively identify

the queried object's numeric identifier in the image. Using this target number, we derive a sequence of precise coordinates for the target. These coordinates, in conjunction with the relevant depth data, are used to generate the 3D point cloud  $\mathcal{P}_q$  of the target.

To optimally select a position that facilitates easy access to the target, we employ a systematic technique for collecting information about the area surrounding the queried object. Initially, the robot is positioned to directly face the target. It then rotates by an angle  $\alpha_0=30^\circ$  to both the left and right, during which it captures both image and depth data. The robot is subsequently tilted downward by a specified angle  $\alpha_1=60^\circ$ , and undergoes additional rotations of  $\alpha_0$  to the left and right. This sequence enhances the collection of comprehensive image and depth data. Utilizing the accumulated images and depth data, the robot constructs a detailed point cloud  $\mathcal P$  in the vicinity of the target.

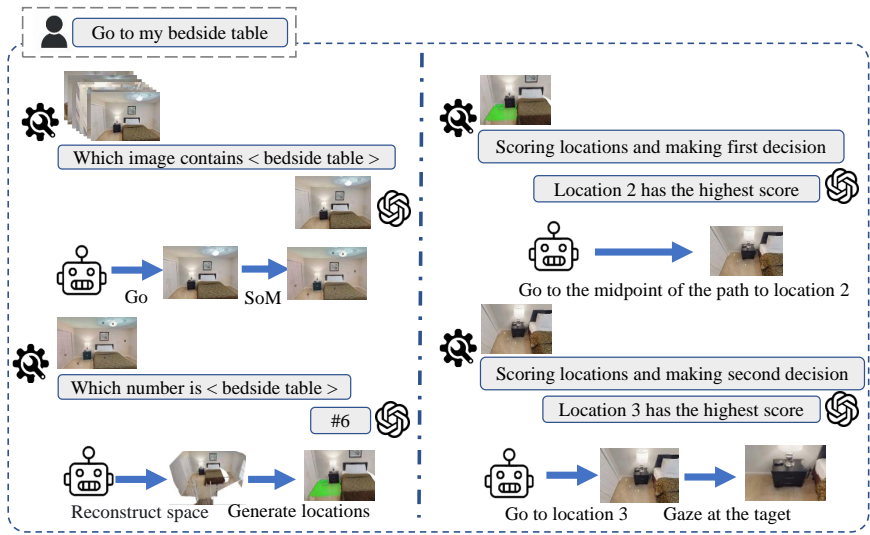


**Figure 3:** Assistive process of GPT-4V in Navi2Gaze. During navigation, GPT-4V sequentially performs scene selection, objective identification, and a two-step decision-making process for gazing target.

#### 3.3 Generation of Location Candidates

Numerous positions in proximity to the target object are accessible. Given the object's orientation attributes, such as the direction in which a refrigerator door opens or a drawer extends, only a subset of these positions are considered optimal for robotic manipulation. We propose a methodology for generating candidate regions, as shown in Figure 4, thereby enabling more informed decision-making in subsequent phases.

Various point cloud data are projected onto the floor plane. The ground's point cloud  $\mathcal{P}_g$ , can be extracted from  $\mathcal{P}$  using a plane extraction algorithm RANSAC. Let  $c_q$  represent the center, and  $r_q$  the radius, of the 2D projection of  $\mathcal{P}_q$  on the ground. On the ground, we construct a 2D square grid map  $\mathcal{M}_s$  with an edge length of  $r_q+1$ , a resolution of 1 cm, and centered at  $c_q$ . We then project the non-ground point cloud, the ground point cloud  $\mathcal{P}_g$ , and the queried object point cloud  $\mathcal{P}_q$  onto this grid map. Each grid can assume one of four possible values:  $\emptyset$  signifies no projection point; 0 indicates an obstacle point; 1 represents an available ground point; 2 denotes the queried object point (a special type of obstacle). The hierarchy of these values, from highest to lowest priority, is: 2, 0, 1,  $\emptyset$ . Priority here implies replaceability—for instance, if a grid initially valued at 0 receives a projection of 2, it is updated to 2; otherwise, it remains unchanged.

To ensure the robot is oriented correctly towards the target, we generate K circular candidate regions  $\{\mathcal{R}_i\}_1^K$ , each with a radius  $r_r$ , around the 2D projection of the queried object on  $\mathcal{M}_s$ . We initiate by establishing a new grid on  $\mathcal{M}_s$  at a resolution of  $r_r/3$ , utilizing the grid vertices as initial centers for the circles. Subsequently, circles are excluded if their minimum distance to the queried object points

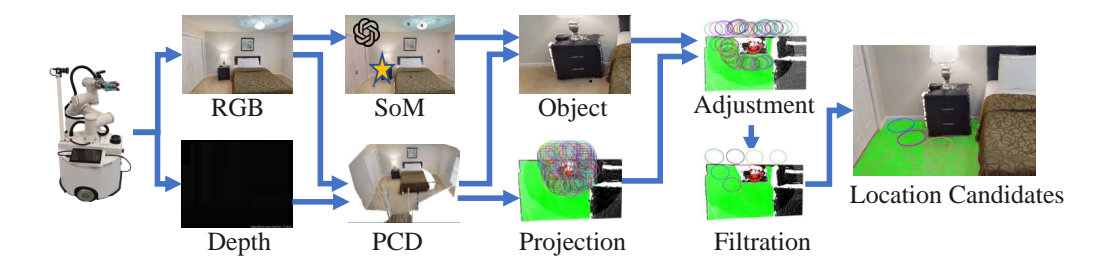


**Figure 4:** Method for Generating Candidate Regions. The robot fuses RGB images with depth images to generate point cloud near the object, utilizing the SoM method for object recognition and segmentation. Point cloud data is projected onto a 2D floor plane. Candidate regions are generated and subsequently refined through adaptive adjustment and selection, resulting in the final candidate regions.

on  $\mathcal{M}_s$  falls below  $r_r/2$  or exceeds  $3r_r/2$ . We categorize different types of 2D points on  $\mathcal{M}_s$  into distinct octrees[38], which facilitates the computation of distances. Following this, we pinpoint the nearest 2D projection point of the queried object to each of the remaining circles and ascertain the directional vector from the circle center to this nearest point. Each circle is then repositioned along this vector to ensure its separation from 2D obstacle points exceeds  $r_r$  marginally. In the final phase, a circle is selected at random, and any overlapping circles are removed. This circle is retained as a candidate, and the process of selecting and retaining the closest non-overlapping circle continues until no circles are left. The circles that are ultimately retained fulfill the aforementioned criteria and are thus designated as the circular candidate regions.

# 3.4 Sequential Decisions for Gazing objects

Guiding the robot to the optimal region and orientation near the target is crucial for reducing the motion gap between robotic navigation and manipulation. To address this problem, we propose a two-step decision-making method designed to facilitate target gazing by robots. The candidate regions are projected onto the image plane with numeric markers, utilizing the cognitive capabilities of the VLM for analytical assessment. In the first step, we input the image containing candidate regions into the VLM for scoring to select the most promising circle. Subsequently, a path to the center of this circle is generated, and the robot is navigated to the midpoint of this path. In the second step, we re-project the candidate regions onto the current image, leveraging the VLM for a second analysis to select the final region. Upon arriving at the final region, the robot rotates to face the target object, thereby accomplishing target gazing.

# 4 System Evaluation

In this section, we comprehensively evaluate our method through simulation to demonstrate its effectiveness relative to baseline methods. Our experiments demonstrate that our method significantly outperforms existing LLM-based navigation algorithms, attributed to the integration of high-quality scores used as navigation heuristics.

#### 4.1 Simulation Setup

**Experimental setup:** Our experiments are conducted on Habitat simulator[39] with the large-scale indoor dataset HM3D v0.2[40]. We collected RGB-D frames from nine different scenes, using a camera height of 1.5 meters and image resolution of  $1080 \times 720$ . Additionally, we documented the camera pose for each frame. We evaluate the performance of Navi2Gaze on the task of object-goal navigation, leveraging insights from the Habitat ObjectNav Challenge [41].

**Evaluation Metrics:** We follow [42] to evaluate our method using Success Rate (SR), Success weighted by Path Length (SPL), and Distance to Goal (DTG). SR is defined as  $\frac{1}{N}\sum_{i=1}^{N}S_i$  and SPL is defined as  $\frac{1}{N}\sum_{i=1}^{N}S_i\frac{l_i}{max(l_i,p_i)}$ , where N is the number of episodes,  $S_i$  is binary indicator of

success in episode i,  $l_i$  is the shortest path length between the start position and the goal,  $p_i$  is the path length of the current episode i. DTG represents the separation between the agent and the goal at the conclusion of the episode. Additionally, to assess the robot's orientation relative to the target object, we introduce the Orientation Toward Goal (OTG) metric. OTG measures the angle between the robot's orientation and the target's optimal operational orientation. Given our focus on ensuring that the robot not only navigates to the proximity of the object but also aligns itself with the correct orientation towards the object, we have redefined the SR, DTG, and OTG in Appendix A.

**Baselines:** We evaluate Navi2Gaze against three baseline methods: VLMaps[13], L3MVN [32], and SemExp[43]. By combining GPT-3 and CLIP, VLMaps translates natural language instructions into a sequence of open-vocabulary goals, directly localized in the map. L3MVN builds the environment map and selects the long-term goal based on the frontiers with the inference of VLMs to achieve efficient exploration and searching. SemExp builds an episodic semantic map and uses it to explore the environment efficiently based on the goal object category.

#### 4.2 Comparison Experiment

We have designed two types of experiments to evaluate the performance of object navigation. Detailed configurations and prompts for these experiments are available in Appendix A and Appendix C, respectively. In the first experiment, the initial positions of the robot are randomly selected, and

Method	Scene A			Scene B		Scene C		Scene D			Scene E			Scene F				
	SR	DTG	OTG	SR	DTG	OTG	SR	DTG	OTG	SR	DTG	OTG	SR	DTG	OTG	SR	DTG	OTG
SemExp	0.10	0.62	18.57	0.09	0.53	10.41	0.13	0.81	21.77	0.17	0.67	22.22	0.25	1.00	14.89	0.09	1.14	58.18
L3MVN	0.17	0.87	10.51	0.28	0.39	11.17	0.42	0.61	20.80	0.33	0.66	28.65	0.38	0.87	12.74	0.28	2.27	43.54
VLMaps	0.27	1.77	43.67	0.61	0.57	37.71	0.34	1.81	41.00	0.44	2.08	49.05	0.00	1.05	80.39	0.61	0.78	45.07
Navi2Gaze	0.56	0.26	15.60	0.59	0.26	7.76	0.85	0.19	11.73	0.71	0.34	22.98	0.60	0.34	21.78	0.33	0.66	46.15

**Table 1:** Navi2Gaze consistently outperforms all baseline methods in randomly selected HM3D scenes with randomly chosen initial poses.

all objects available in the scenes are used for the baselines. The outcomes of these experiments are presented in Table 1. Our observations indicate that Navi2Gaze consistently outperforms all baselines. Both SemExp and L3MVN are vulnerable during the map-building process because obstacles are frequently introduced into the 2D map, preventing the robots from finding available paths to the objects. Occasionally, they exhibit lower OTG values because positions that are slightly farther from the objects are more likely to offer better orientations. VLMaps plans paths and navigates to objects based solely on the initially provided RGB-D frames with poses, thereby overlooking obstacles not covered in the initial frames. Consequently, the paths delineated by VLMaps frequently lead through walls, resulting in erroneous positions relative to the target objects. An example of the final observations is illustrated in Figure 5, additional visualization results are available in Appendix B.

Method		Sce	ene G			Sce	ene H		Scene I			
	SR	SPL	DTG	OTG	SR	SPL	DTG	OTG	SR	SPL	DTG	OTG
VLMaps Navi2Gaze								68.92 <b>32.77</b>				

**Table 2:** Navi2Gaze consistently achieves superior performance over VLMaps in randomly selected HM3D scenes, demonstrating significantly high SR values, particularly when the initial poses are positioned at the sides of the objects.

In the second experiment, we select the initial poses of the robots at the side or back of the objects. This configuration demonstrates that our method effectively guides the robots to the correct positions with the appropriate orientation, thereby validating the efficacy of our visual prompting and scoring mechanisms. We mainly compare Navi2Gaze with VLMaps in these experiments and the results are shown in Table 2. Our findings indicate that with appropriate visual prompts, VLMs can effectively

determine the optimal positions for the robots, resulting in our method significantly outperforming VLMaps across all metrics.



**Figure 5:** The visualization of final observations from four navigation methods targeting a chair reveals that Navi2Gaze effectively directs the robot to the front of the chair. Conversely, other methods frequently result in the robot approaching the chair from the back or side.

#### 4.3 Ablation Studies

To assess the relative importance of the various modules within our framework, we have performed the ablations using the HM3D dataset: Directly Navigating to the Target (Navi2Gaze-DNT), without Reconstruction of Task-aware Space (Navi2Gaze-w/o RTS), One-step Goal Decision (Navi2Gaze-OGD). The results in TABLE 3 show that our complete framework achieves the optimal performance, and the scoring mechanism and sequential decisions are crucial for achieving good performance. Our findings indicate that direct navigation to the target often fails, resulting in a significantly larger DTG. Without a reconstruction of task-aware space, the robot struggles to accurately recognize the ground due to insufficient information. Furthermore, replacing sequential decisions with a single-step goal decision leads to a decrease in both SR and SPL.

	SR	SPL	DTG	OTG
Navi2Gaze	0.76	0.46	0.56	11.58
Navi2Gaze-DNT	0.02	0.01	1.24	26.19
Navi2Gaze-OGD	0.55	0.37	0.85	23.37
Navi2Gaze-w/o RTS	0.27	0.20	1.22	49.23

**Table 3:** Results from ablation studies in HM3D scenes demonstrate that Navi2Gaze, when implemented with its complete framework, ensures optimal performance.

# 5 Conclusion

**Summary:** We introduce Navi2Gaze, a method that leverages vision language models to interpret and guide robots towards achieving goals with precise positions and orientations. The fundamental insight of our research is that while VLMs offer rich semantic understanding, their suggestions for navigational tasks should be employed as heuristics rather than definitive plans. We have developed a technique to extract heuristic scores from language models by proper visual prompts, which are subsequently integrated into a navigation algorithm. This heuristic-based approach enables more effective navigation, ensuring robots reach their goals with the desired accuracy in both position and orientation.

Limitations and future work: While our experiments support our main hypothesis, they have some limitations. First, our tests are only in simulated indoor environments. Using real robots in the real world could give different results, especially in accurately determining their poses. Future research could explore integrating Simultaneous Localization and Mapping (SLAM) for real robot use. Second, our approach relies on cloud-based VLMs. Conducting experiments via API calls to VLMs requires a stable internet connection, which limits real-world applications. We expect that ongoing improvements in VLM quantization for edge deployment and faster inference will help address this issue.

#### References

- [1] S. Yenamandra, A. Ramachandran, K. Yadav, A. S. Wang, M. Khanna, T. Gervet, T.-Y. Yang, V. Jain, A. Clegg, J. M. Turner, Z. Kira, M. Savva, A. X. Chang, D. S. Chaplot, D. Batra, R. Mottaghi, Y. Bisk, and C. Paxton. Homerobot: Open-vocabulary mobile manipulation. In *7th Annual Conference on Robot Learning*, 2023. URL https://openreview.net/forum?id=b-cto-fetlz.
- [2] A. Saxena, J. Driemeyer, and A. Y. Ng. Learning 3-d object orientation from images. In 2009 IEEE International Conference on Robotics and Automation, pages 794–800, 2009. doi: 10.1109/ROBOT.2009.5152855.
- [3] Z. He, N. Chavan-Dafle, J. Huh, S. Song, and V. Isler. Pick2place: Task-aware 6dof grasp estimation via object-centric perspective affordance. In 2023 IEEE International Conference on Robotics and Automation (ICRA), pages 7996–8002. IEEE, 2023.
- [4] M. Sundermeyer, Z.-C. Marton, M. Durner, M. Brucker, and R. Triebel. Implicit 3d orientation learning for 6d object detection from rgb images. In *The European Conference on Computer Vision (ECCV)*, September 2018.
- [5] K. Wada, S. James, and A. J. Davison. Reorientbot: Learning object reorientation for specific-posed placement. In 2022 International Conference on Robotics and Automation (ICRA), pages 8252–8258, 2022.
- [6] Y. Hai, R. Song, J. Li, and Y. Hu. Shape-constraint recurrent flow for 6d object pose estimation. In Proceedings of the IEEE/CVF Conference on Computer Vision and Pattern Recognition, pages 4831–4840, 2023.
- [7] B. Wen, J. Tremblay, V. Blukis, S. Tyree, T. Müller, A. Evans, D. Fox, J. Kautz, and S. Birchfield. Bundlesdf: Neural 6-dof tracking and 3d reconstruction of unknown objects. In *Proceedings of the IEEE/CVF Conference on Computer Vision and Pattern Recognition*, pages 606–617, 2023.
- [8] M. Kokic, D. Kragic, and J. Bohg. Learning task-oriented grasping from human activity datasets. *IEEE Robotics and Automation Letters*, 5(2):3352–3359, 2020.
- [9] T. Brown, B. Mann, N. Ryder, M. Subbiah, J. D. Kaplan, P. Dhariwal, A. Neelakantan, P. Shyam, G. Sastry, A. Askell, et al. Language models are few-shot learners. *Advances in neural information processing systems*, 33:1877–1901, 2020.
- [10] OpenAI. Gpt-4 technical report, 2024.
- [11] A. Chowdhery, S. Narang, J. Devlin, M. Bosma, G. Mishra, A. Roberts, P. Barham, H. W. Chung, C. Sutton, S. Gehrmann, et al. Palm: Scaling language modeling with pathways. *arXiv* preprint arXiv:2204.02311, 2022.
- [12] A. Majumdar, G. Aggarwal, B. Devnani, J. Hoffman, and D. Batra. Zson: Zeroshot object-goal navigation using multimodal goal embeddings. In S. Koyejo, S. Mohamed, A. Agarwal, D. Belgrave, K. Cho, and A. Oh, editors, *Advances in Neural Information Processing Systems*, volume 35, pages 32340–32352. Curran Associates, Inc., 2022. URL https://proceedings.neurips.cc/paper\_files/paper/2022/file/d0b8f0c8f79d3a621af945cafb669f4b-Paper-Conference.pdf.
- [13] C. Huang, O. Mees, A. Zeng, and W. Burgard. Visual language maps for robot navigation. In 2023 IEEE International Conference on Robotics and Automation (ICRA), pages 10608–10615, 2023. doi:10.1109/ICRA48891.2023.10160969.
- [14] W. Cai, S. Huang, G. Cheng, Y. Long, P. Gao, C. Sun, and H. Dong. Bridging zero-shot object navigation and foundation models through pixel-guided navigation skill, 2023.

- [15] L. H. Li, P. Zhang, H. Zhang, J. Yang, C. Li, Y. Zhong, L. Wang, L. Yuan, L. Zhang, J.-N. Hwang, K.-W. Chang, and J. Gao. Grounded language-image pre-training. In *Proceedings of the IEEE/CVF Conference on Computer Vision and Pattern Recognition (CVPR)*, pages 10965–10975, June 2022.
- [16] A. Radford, J. W. Kim, C. Hallacy, A. Ramesh, G. Goh, S. Agarwal, G. Sastry, A. Askell, P. Mishkin, J. Clark, G. Krueger, and I. Sutskever. Learning transferable visual models from natural language supervision. In M. Meila and T. Zhang, editors, *Proceedings of the 38th International Conference on Machine Learning*, volume 139 of *Proceedings of Machine Learning Research*, pages 8748–8763. PMLR, 18–24 Jul 2021.
- [17] J. Yang, H. Zhang, F. Li, X. Zou, C. Li, and J. Gao. Set-of-mark prompting unleashes extraor-dinary visual grounding in gpt-4v, 2023. URL https://arxiv.org/abs/2310.11441.
- [18] L. Yang, Y. Wang, X. Li, X. Wang, and J. Yang. Fine-grained visual prompting. In A. Oh, T. Naumann, A. Globerson, K. Saenko, M. Hardt, and S. Levine, editors, *Advances in Neural Information Processing Systems*, volume 36, pages 24993–25006. Curran Associates, Inc., 2023. URL https://proceedings.neurips.cc/paper\_files/paper/2023/file/4e9fa6e716940a7cfc60c46e6f702f52-Paper-Conference.pdf.
- [19] Y. Yao, A. Zhang, Z. Zhang, Z. Liu, T.-S. Chua, and M. Sun. Cpt: Colorful prompt tuning for pre-trained vision-language models. *AI Open*, 5:30–38, 2024.
- [20] X. Gu, T.-Y. Lin, W. Kuo, and Y. Cui. Open-vocabulary object detection via vision and language knowledge distillation. *arXiv preprint arXiv:2104.13921*, 2021.
- [21] B. Chen, F. Xia, B. Ichter, K. Rao, K. Gopalakrishnan, M. S. Ryoo, A. Stone, and D. Kappler. Open-vocabulary queryable scene representations for real world planning. In 2023 IEEE International Conference on Robotics and Automation (ICRA), pages 11509–11522, 2023. doi: 10.1109/ICRA48891.2023.10161534.
- [22] B. Li, K. Q. Weinberger, S. Belongie, V. Koltun, and R. Ranftl. Language-driven semantic segmentation. *arXiv preprint arXiv:2201.03546*, 2022.
- [23] A. Shtedritski, C. Rupprecht, and A. Vedaldi. What does clip know about a red circle? visual prompt engineering for vlms. In *Proceedings of the IEEE/CVF International Conference on Computer Vision (ICCV)*, pages 11987–11997, October 2023.
- [24] S. Subramanian, W. Merrill, T. Darrell, M. Gardner, S. Singh, and A. Rohrbach. Reclip: A strong zero-shot baseline for referring expression comprehension. arXiv preprint arXiv:2204.05991, 2022.
- [25] X. Zou, J. Yang, H. Zhang, F. Li, L. Li, J. Wang, L. Wang, J. Gao, and Y. J. Lee. Segment everything everywhere all at once. In A. Oh, T. Naumann, A. Globerson, K. Saenko, M. Hardt, and S. Levine, editors, *Advances in Neural Information Processing Systems*, volume 36, pages 19769–19782. Curran Associates, Inc., 2023. URL https://proceedings.neurips.cc/paper\_files/paper/2023/file/ 3ef61f7e4afacf9a2c5b71c726172b86-Paper-Conference.pdf.
- [26] A. Kirillov, E. Mintun, N. Ravi, H. Mao, C. Rolland, L. Gustafson, T. Xiao, S. Whitehead, A. C. Berg, W.-Y. Lo, P. Dollar, and R. Girshick. Segment anything. In *Proceedings of the IEEE/CVF International Conference on Computer Vision (ICCV)*, pages 4015–4026, October 2023.
- [27] H. Dai, C. Ma, Z. Liu, Y. Li, P. Shu, X. Wei, L. Zhao, Z. Wu, D. Zhu, W. Liu, et al. Samaug: Point prompt augmentation for segment anything model. *arXiv preprint arXiv:2307.01187*, 2023.

- [28] L. Tang, H. Xiao, and B. Li. Can sam segment anything? when sam meets camouflaged object detection. *arXiv preprint arXiv:2304.04709*, 2023.
- [29] R. Zhang, Z. Jiang, Z. Guo, S. Yan, J. Pan, X. Ma, H. Dong, P. Gao, and H. Li. Personalize segment anything model with one shot. *arXiv* preprint arXiv:2305.03048, 2023.
- [30] F. Rajič, L. Ke, Y.-W. Tai, C.-K. Tang, M. Danelljan, and F. Yu. Segment anything meets point tracking. *arXiv preprint arXiv:2307.01197*, 2023.
- [31] D. Driess, F. Xia, M. S. M. Sajjadi, C. Lynch, A. Chowdhery, B. Ichter, A. Wahid, J. Tompson, Q. Vuong, T. Yu, W. Huang, Y. Chebotar, P. Sermanet, D. Duckworth, S. Levine, V. Vanhoucke, K. Hausman, M. Toussaint, K. Greff, A. Zeng, I. Mordatch, and P. Florence. Palm-e: an embodied multimodal language model. In *Proceedings of the 40th International Conference on Machine Learning*, ICML'23. JMLR.org, 2023.
- [32] B. Yu, H. Kasaei, and M. Cao. L3mvn: Leveraging large language models for visual target navigation. In 2023 IEEE/RSJ International Conference on Intelligent Robots and Systems (IROS). IEEE, Oct. 2023. doi:10.1109/iros55552.2023.10342512. URL http://dx.doi.org/ 10.1109/IROS55552.2023.10342512.
- [33] K. Zhou, K. Zheng, C. Pryor, Y. Shen, H. Jin, L. Getoor, and X. E. Wang. Esc: exploration with soft commonsense constraints for zero-shot object navigation. In *Proceedings of the 40th International Conference on Machine Learning*, ICML'23. JMLR.org, 2023.
- [34] V. S. Dorbala, J. F. Mullen, and D. Manocha. Can an embodied agent find your "cat-shaped mug"? Ilm-based zero-shot object navigation. *IEEE Robotics and Automation Letters*, 9(5): 4083–4090, 2024. doi:10.1109/LRA.2023.3346800.
- [35] D. Shah, M. Equi, B. Osinski, F. Xia, B. Ichter, and S. Levine. Navigation with large language models: Semantic guesswork as a heuristic for planning. In 7th Annual Conference on Robot Learning, 2023. URL https://openreview.net/forum?id=PsV65r0itpo.
- [36] J. Chen, G. Li, S. Kumar, B. Ghanem, and F. Yu. How to not train your dragon: Training-free embodied object goal navigation with semantic frontiers, 2023.
- [37] D. Shah, B. Osiński, S. Levine, et al. Lm-nav: Robotic navigation with large pre-trained models of language, vision, and action. In *Conference on robot learning*, pages 492–504. PMLR, 2023.
- [38] J. Zhu, H. Li, S. Wang, Z. Wang, and T. Zhang. i-octree: A fast, lightweight, and dynamic octree for proximity search, 2023.
- [39] M. Savva, A. Kadian, O. Maksymets, Y. Zhao, E. Wijmans, B. Jain, J. Straub, J. Liu, V. Koltun, J. Malik, D. Parikh, and D. Batra. Habitat: A platform for embodied ai research. In *Proceedings of the IEEE/CVF International Conference on Computer Vision (ICCV)*, October 2019.
- [40] S. K. Ramakrishnan, A. Gokaslan, E. Wijmans, O. Maksymets, A. Clegg, J. M. Turner, E. Undersander, W. Galuba, A. Westbury, A. X. Chang, M. Savva, Y. Zhao, and D. Batra. Habitat-matterport 3d dataset (HM3d): 1000 large-scale 3d environments for embodied AI. In *Thirty-fifth Conference on Neural Information Processing Systems Datasets and Benchmarks Track (Round 2)*, 2021. URL https://openreview.net/forum?id=-v40uqNs5P.
- [41] K. Yadav, S. K. Ramakrishnan, J. Turner, A. Gokaslan, O. Maksymets, R. Jain, R. Ramrakhya, A. X. Chang, A. Clegg, M. Savva, E. Undersander, D. S. Chaplot, and D. Batra. Habitat challenge 2022. https://aihabitat.org/challenge/2022/, 2022.
- [42] P. Anderson, A. Chang, D. S. Chaplot, A. Dosovitskiy, S. Gupta, V. Koltun, J. Kosecka, J. Malik, R. Mottaghi, M. Savva, et al. On evaluation of embodied navigation agents. *arXiv* preprint *arXiv*:1807.06757, 2018.

[43] D. S. Chaplot, D. P. Gandhi, A. Gupta, and R. R. Salakhutdinov. Object goal navigation using goal-oriented semantic exploration. In H. Larochelle, M. Ranzato, R. Hadsell, M. Balcan, and H. Lin, editors, *Advances in Neural Information Processing Systems*, volume 33, pages 4247–4258. Curran Associates, Inc., 2020. URL https://proceedings.neurips.cc/paper\_files/paper/2020/file/2c75cf2681788adaca63aa95ae028b22-Paper.pdf.

# A Implementation Details

In this challenge, the agent operates within a simulated environment featuring photorealistic graphics and is tasked with locating a queried object from one of ten categories, such as "toilet," "bed," and "couch." In these environments, the robot is required to navigate in a continuous environment with actions:  $\{stop, move\_forward, turn\_left, turn\_right, look\_up, look\_down\}$ . The forward distance is set to 0.1m, and the rotation angle is set to 1 degrees. The OTG and DTG are defined in Figure 6.

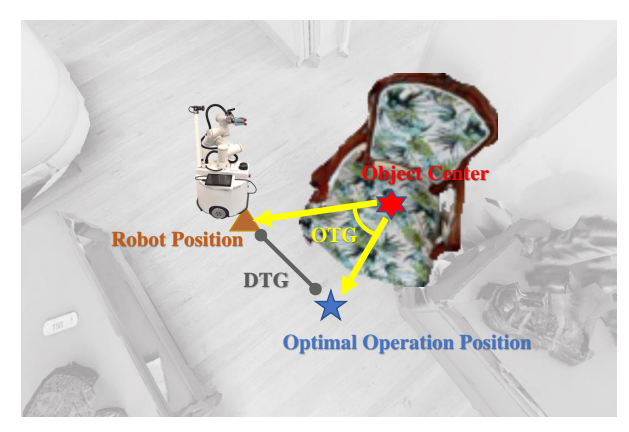
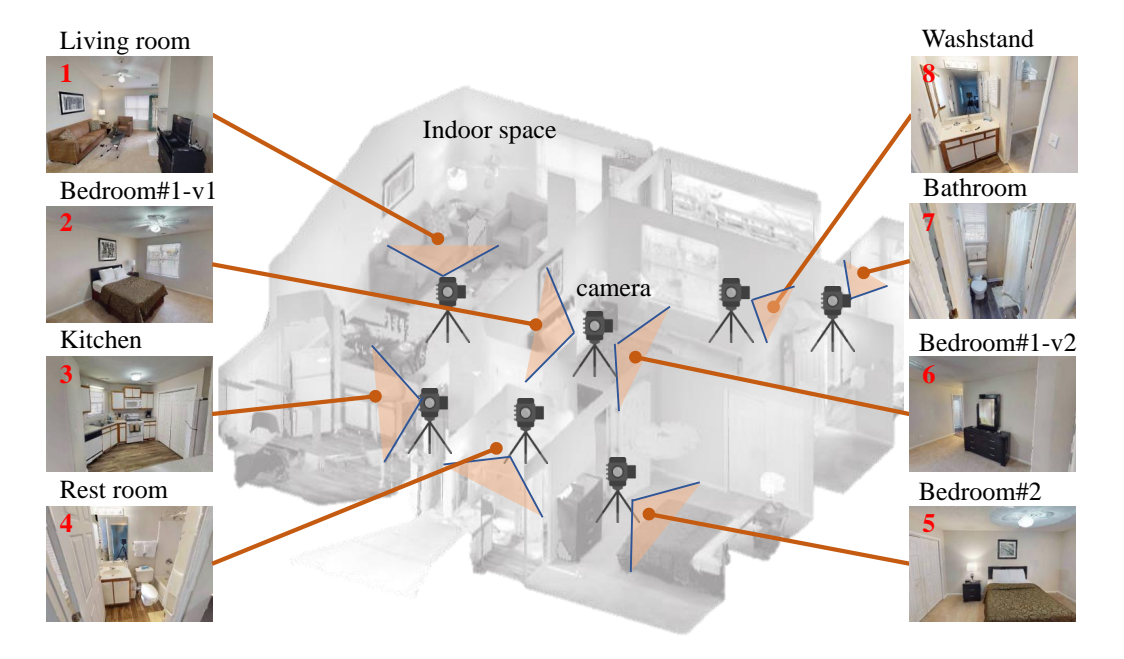


Figure 6: OTG and DTG.

The Navi2Gaze method proposed in this paper requires the collection of indoor scene images, as shown in Figure 7. The robot explores the indoor environment, capturing images of various scenes, recording the locations of the shots, and numbering the images. To achieve a more comprehensive navigation effect, each image aims to include as many objects as possible.



**Figure 7:** Initial acquisition of scene images. The robot conducts explorations of the scene, documenting images of various rooms along with their respective capture locations. Each image is numbered and labeled in the upper left corner.

The nine different scenes used in the simulation are all derived from HM3D v0.2, with their corresponding identification codes shown in Figure 8.



Figure 8: Experimental Scene

We define the angle between the robot's direction and the optimal operating direction of the target as OTG. The optimal operating directions for multiple navigation targets in the nine scenes were manually annotated. Some of the annotation results are shown in the Figure 9.

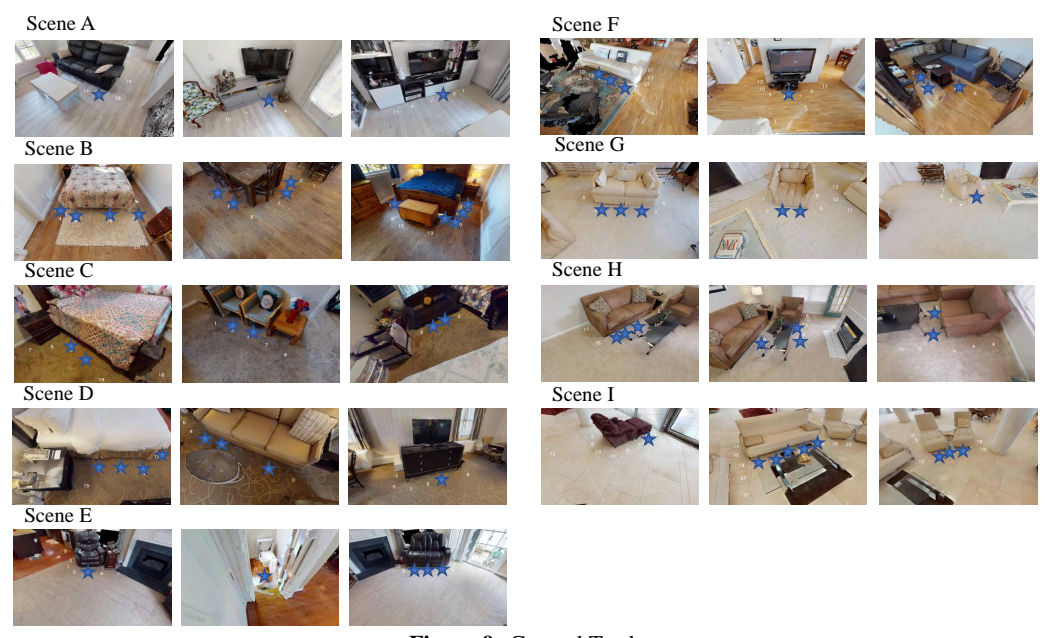


Figure 9: Ground Truth

# **B** Visualization of Navigation Performance

The simulation results of navigating to five other objects using four different methods are compared, as shown in the figure 10. The Navi2Gaze method introduced in this paper enables navigation to the vicinity of the objects while adopting an appropriate posture to gaze at the objects, facilitating subsequent operations by the robot

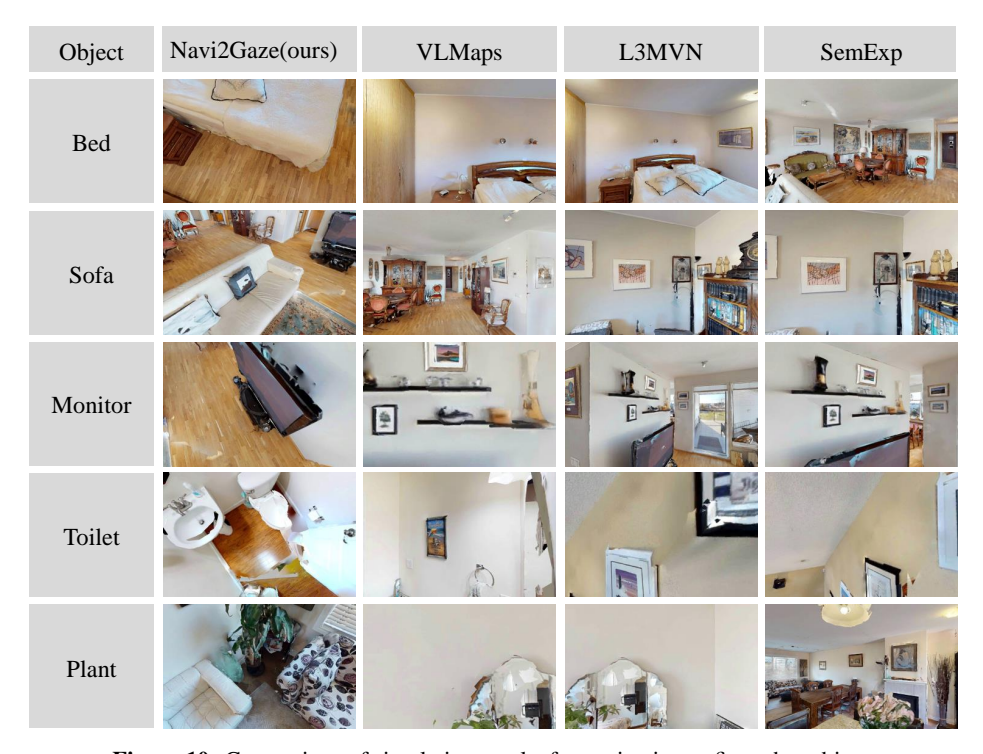


Figure 10: Comparison of simulation results for navigation to five other objects

# C Prompts

# **Parsing Instructions:**

```
question = f"""
I: open the refrigerator. A: [refrigerator, open the refrigerator]
I: navigate to the bed and pick up a pillow, finally go to the painting.
    A: [[green sofa, navigate to the green sofa], [pillow, pick up a pillow]]
I: {language_instr}. A:"""
```

#### **Selecting Image:**

```
user_input_select_image = f"Among these {img_n} images, each labeled with
    a red number in the upper left corner, could you identify which one(
    s) feature a {object_name} and provide the picture number(s)? Then in
    the picture(s) with the {object_name}, please choose a clearest
    picture, please directly tell me the number of the picture you
    selected at last. Please output only one number to me. If you can
    not find, return None."
```

#### **Selecting Segmentation Mask:**

```
user_input_select_seg_mask = f"Please find the {object_name} in the first
  image and tell me the corresponding number on it in the second image
  , the number is best placed on {object_name}. Please output only one
  number to me"
```

# **Selecting Circle:**

user\_input\_ = f"In this image, I have marked certain circles in the image
 with both color and number, which circle do I need go if I want to {
 exe}. Please inform me of its corresponding number. Scoring the
 accessibility of each circle on a scale from 0 to 10, where higher
 scores indicate better accessibility. Each circle should have a
 unique score. Please only return circle numbers with the top 6
 highest scored values."